Supplementary Figure 1. **Nonlinear proliferation in drug-treated and high-density cultured cells.**

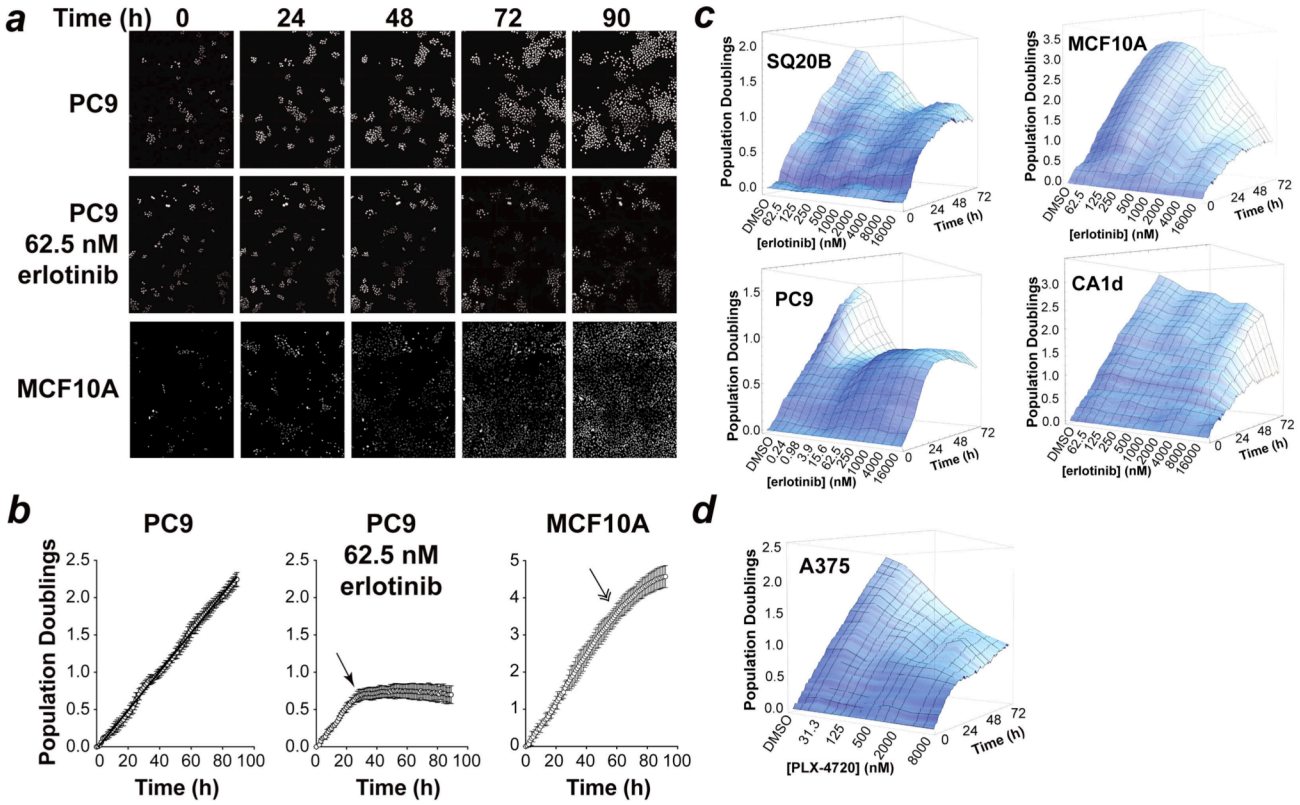

Supplementary Figure 1. **Nonlinear proliferation in drug-treated and high-density cultured cells.** (**a**) Cells expressing histone H2BmRFP were cultured in complete medium (PC9 and MCF10A) or in the presence of erlotinib (as indicated) and analyzed by time-lapse live-cell automated microscopy. Images were obtained at the indicated times from approximately 1 mm^2 within a single well and nuclei are visible in white. Note that only MCF10A cells approach confluence due to their rapid rate of proliferation. (**b**) Proliferation slows in response to erlotinib or at high cell density. Nuclei from replicate wells were counted every hour, normalized for cell number and plotted on a $\log_2$ scale. PC9 cells exhibit linear growth throughout the experiment as indicated by the line overlapping the data (R^2=0.9884). Nonlinearity begins in PC9 cells in response to erlotinib at approximately 24 h (arrow) and in MCF10A cells at high density around 60 h (double arrowhead). Bars at each data point indicate intraexperimental error (standard deviation) from replicate wells. For PC9, *n* = 6; PC9 in erlotinib, *n* = 6; MCF10A, *n* = 2. (**c**) Surface plots of proliferation were obtained from four different cell lines of diverse backgrounds and differing sensitivities to EGFR TKI: i) PC9, an oncogene-addicted human lung adenocarcinoma cell line hypersensitive to erlotinib-like TKI due to an EGFR mutation [1,2]; ii) MCF10A, a non-tumorigenic human mammary epithelial cell line, which is dependent on EGF for proliferation [6]; iii) CA1d, a mutant H-ras-expressing tumorigenic MCF10A derivative [7,8]; and iv) SQ20B, a human laryngeal squamous cell carcinoma cell line with genomic amplification of EGFR [9]. (**d**) Surface plot of the response of A375 cells to the Raf inhibitor PLX-4720. A375 cells are oncogene-addicted melanoma cells containing mutant B-Raf that are highly sensitive to Raf inhibition [10].

Supplementary Figure 2. **Nonlinear proliferation rates.**

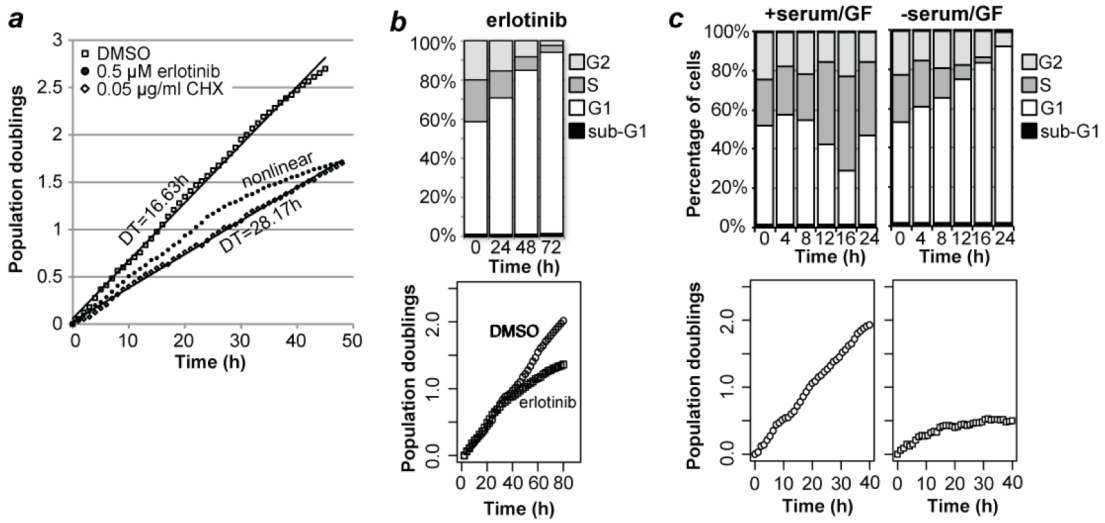

Supplementary Figure 2. **Nonlinear proliferation rates.** (**a**) Proliferation of MCF10A cells grown in the absence of drugs (DMSO vehicle control, *open squares*) or in the presence of the indicated concentrations of erlotinib (*filled circles*) or cycloheximide (CHX; *open diamonds*) are shown. The response to CHX was fit to a line and demonstrates a doubling time (DT) of 28.17 h. In contrast, the response to erlotinib was nonlinear. Data from a single experiment are shown. Linear or nonlinear responses, respectively, were reproduced in at least three independent experiments. (**b**) Erlotinib induces entry into quiescence and nonlinear proliferation rates in PC9 cells. *Upper panel*, PC9 cells were cultured in complete medium with 15.6 nM erlotinib for the indicated times and analyzed by flow cytometry to determine the fraction of cells in each cell cycle compartment based on DNA content. *Lower panel*, cell counts from image stacks at 2-hour intervals are presented on a normalized $\log_2$ scale and indicate population doublings. Vehicle-treated cells (DMSO; open circles) demonstrated linear proliferation whereas erlotinib-treated cell proliferation (open squares) was nonlinear. (**c**) Serum and growth factor (GF) deprivation causes accumulation of cells in G1 and nonlinear effects on proliferation curves. *Upper panel*, MCF10A cells were cultured in complete medium (+serum/GF) or serum and GF-deprived medium (-serum/GF) and analyzed by flow cytometry to determine the fraction of cells in each cell cycle compartment based on DNA content and incorporation of bromodeoxyuridine. The removal of serum and GF results in >95% of cells in G1 after 24 h. *Lower panel*, cells were counted at one-hour intervals. Serum and GF deprivation (open squares) results in a nonlinear proliferation curve whereas in complete medium (open circles) the proliferation is linear. Data from a single experiment are shown. Nonlinear response of serum/GF deprivation was reproduced in at least three independent experiments.

Supplementary Figure 3. **Quiescence-Growth model fits of CA1d cells treated with erlotinib.**

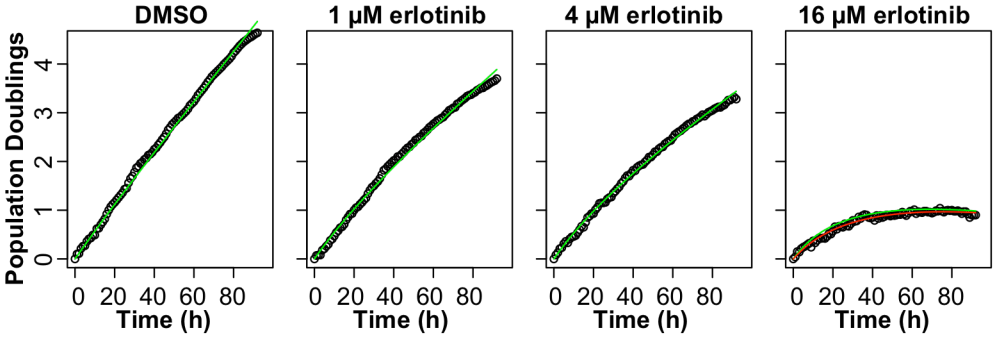

Supplementary Figure 3. **Quiescence-Growth model fits of CA1d cells treated with erlotinib.** Open circles indicate data points from cell counts of CA1d cells exposed to vehicle (DMSO) or erlotinib at specified concentrations for 96 h. Green lines represent the best fit of the Quiescence-Growth model when the division rate (*d*) is fixed to that of the untreated population, $a = 0$, and q is fit by nonlinear least squares regression. The red line in the 16 μM erlotinib panel was obtained by allowing both a and q to be fit. The values of these parameters are shown in **Supplementary Table 1**. For a dynamic visualization of the effects of parameter modulation on population doublings, see **Supplementary Software 1**.

Supplementary Figure 4. **Detection of cell death and division in image sequences.**

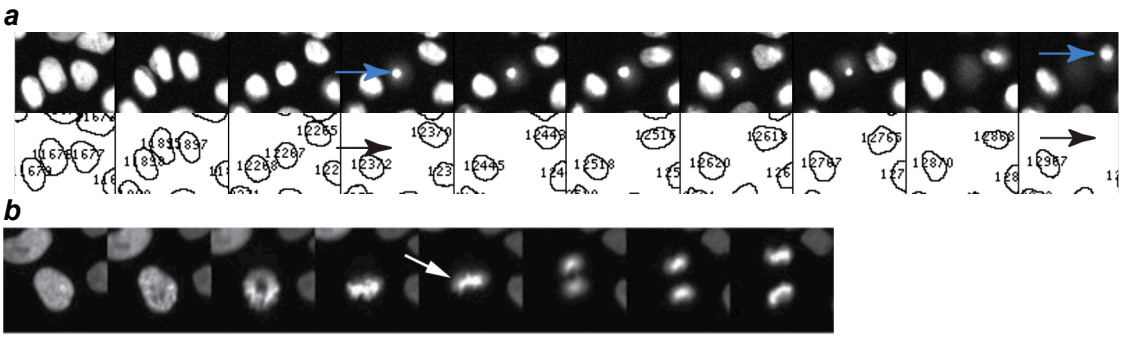

Supplementary Figure 4. **Detection of cell death and division in image sequences.** (**a**) Recognition of cell death based on the reduction of nuclear surface area below threshold for detection. A sequence of images (*upper panel*) is paired with detection output from ImageJ (*lower panel*). Blue arrows indicate nuclei that shrank dramatically from the preceding frame, due to cell death. Black arrows show that the shrunk nuclei are now below the level of detection of ImageJ. Note that ImageJ does not track individual nuclei from frame to frame and, therefore, the nuclear ID is not maintained from image to image. (**b**) Example image sequence demonstrating mitotic events visualized by fluorescence microscopy of nuclei (H2BmRFP expression). Arrow indicates metaphase chromosomes preceding anaphase separation in the following frame.

Supplementary Figure 5. **Intermitotic time distribution fit by an EMG model.**

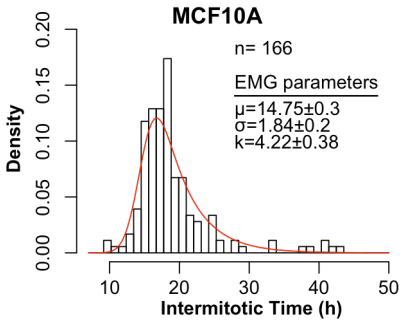

Supplementary Figure 5. **Intermitotic time distribution fit by an EMG model.** An IMT distribution obtained from exponentially proliferating MCF10A cells was fit to an EMG and the best-fit parameters are indicated. Using the method of Powell [3], all parameters (μ, σ and k) are used to determine the division rate of the population (parameter d in the Quiescence-Growth model).

Supplementary Figure 6. **EMG parameters are differentially affected by drugs.**

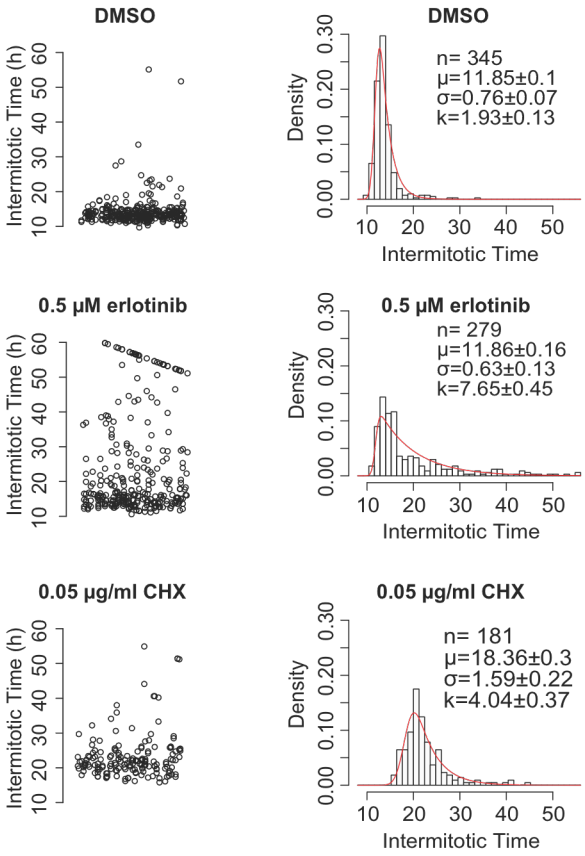

Supplementary Figure 6. **EMG parameters are differentially affected by drugs.** Intermitotic times of MCF10A cells treated with vehicle (DMSO) have a relatively compact distribution with a small rightward skew. Upon treatment with erlotinib, the rightward skew increases substantially and is captured by the increase of the *k* parameter. Cycloheximide (CHX) increases the intermitotic times of all of the cells in the population and is captured primarily by the increased value of the EMG parameter *μ*. These single-cell data correspond to the proliferation curves (population-level data) shown in **Supplementary Figure 2a**.

Supplementary Figure 7. **Ki-67 intensity decreases in erlotinib-treated PC9 cells.**

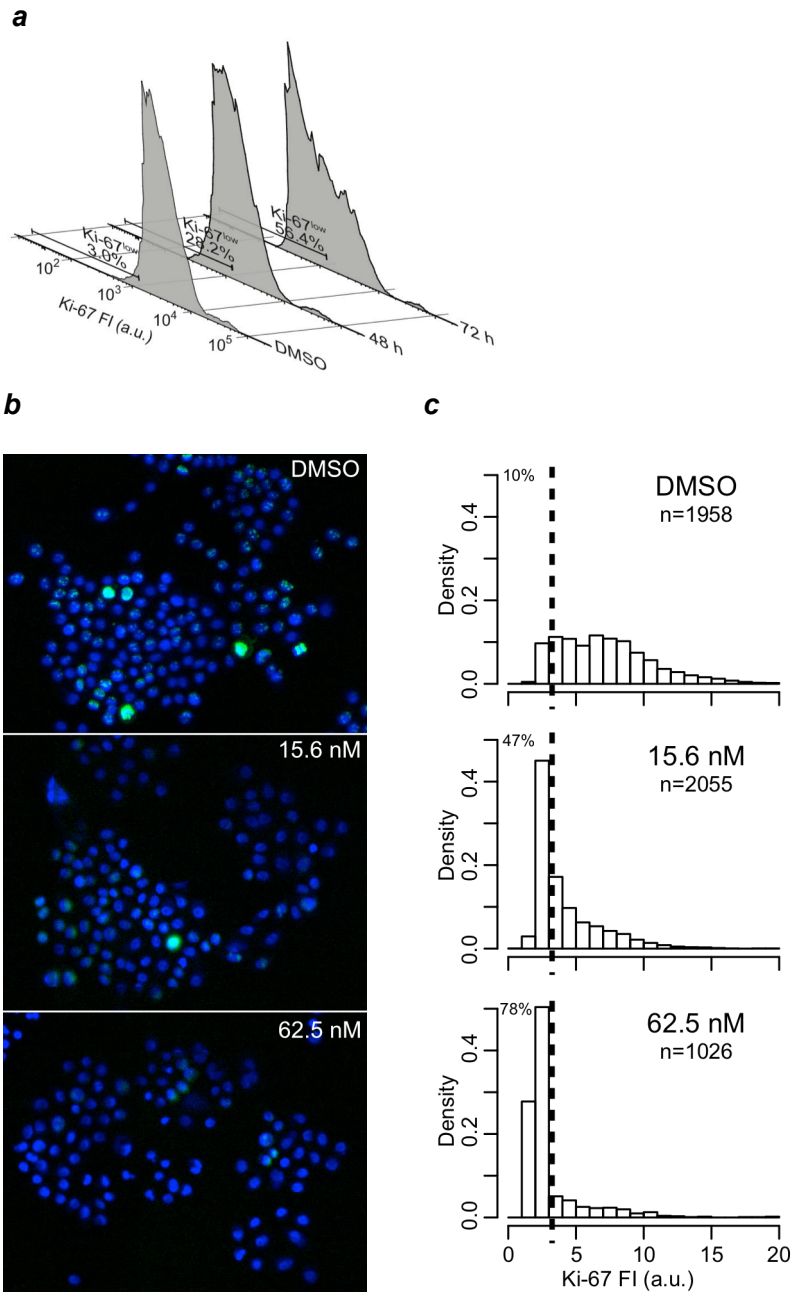

Supplementary Figure 7. **Ki-67 intensity decreases in erlotinib-treated PC9 cells.** (**a**) PC9 cells were treated with 15.6 nM erlotinib for the indicated amounts of time, fixed and analyzed for expression level of Ki-67 by flow cytometry. The Ki-67^{low} population was determined using an arbitrarily chosen threshold intensity value of ~1500 and is indicated for each histogram. Note that the Ki-67 level shifts downward but does not disappear as previously described [4]. The fractions of quiescent cells in each of these conditions as predicted by the parameterization of the Quiescence-Growth model from single cell data shown in Figure 4 of the main text are 4%, 43% and 57%, respectively, which approximates the Ki-67^{low} population shown. (**b**) PC9 cells were treated with the indicated concentrations of erlotinib or DMSO for ~72 h, fixed with paraformaldehyde, immunostained for Ki-67 (green), counterstained with Hoechst 33342 (blue) and imaged by fluorescence microscopy. Smaller subregions of obtained images are shown. (**c**) All cells in the full images from which the subregions in (*b*) were derived were quantified for Ki-67 intensity and normalized to nuclear area. A density plot of the distribution of normalized intensity values is shown. The vertical dashed line indicates the threshold value arbitrarily set to 3 to approximate the fractions of Ki-67^{low} cells in DMSO-treated cells in *a* above. Fractions of cells with less than these threshold values of Ki-67 intensity are indicated. The predicted quiescent fractions at this time (based on the model fits described in **Figure 4** of the main text) are 4%, 64% and 91% for DMSO, 15.6 nM erlotinib and 62.5 nM erlotinib, respectively.

Supplementary Figure 8. **PLX-4720 induces nuclear p27 expression in A375 cells.**

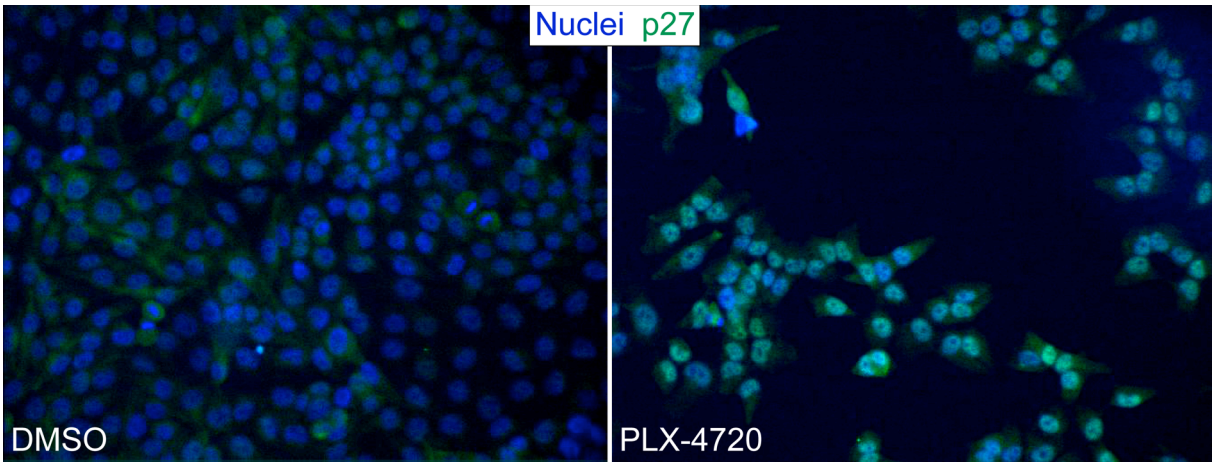

Supplementary Figure 8. **PLX-4720 induces nuclear p27 expression in A375 cells.** A375 cells treated with DMSO (left) or 16 μM PLX-4720 (right) for 72 h were immunostained for p27 (green). The expressed histone H2B-mRFP was used to detect nuclei (blue). Note faint diffuse staining in the cytoplasm of DMSO-treated cells. The significant overlap of the green and blue channels in the PLX-4720-treated cells indicates strong expression and nuclear localization of p27. The decreased number of cells treated with PLX-4720 correlates with increased levels of nuclear p27 and is indicative of cell cycle arrest.

Supplementary Figure 9. **Analysis of PC9 cell survival in erlotinib from Supplementary Video 1.**

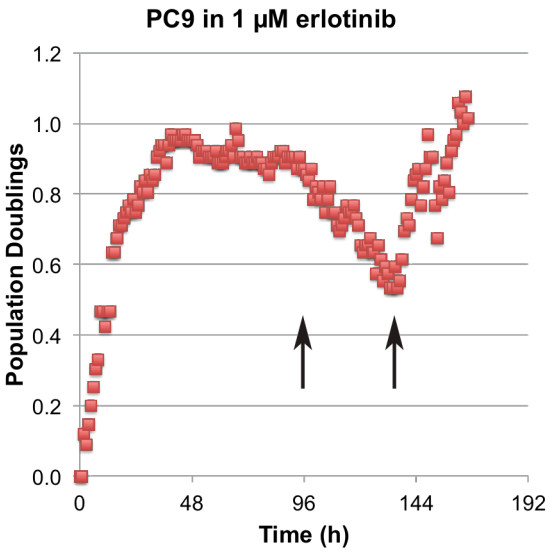

Supplementary Figure 9. **Analysis of PC9 cell survival in erlotinib from Supplementary Video 1.** PC9 exposed to 1 μM erlotinib for 4 days resume proliferation upon erlotinib removal, indicating quiescent cells are viable. The data for this experiment is shown in **Supplementary Video 1**. Nuclei were quantified and plotted on a normalized log2 scale (Population Doublings). Arrows indicate time of erlotinib removal by medium replacement at 96 and 140 h. (Note that the rate of proliferation after erlotinib withdrawal returned to pretreatment levels.)

Supplementary Figure 10. **Fractional Proliferation of primary human SCC cells shown in Supplementary Video 3.**

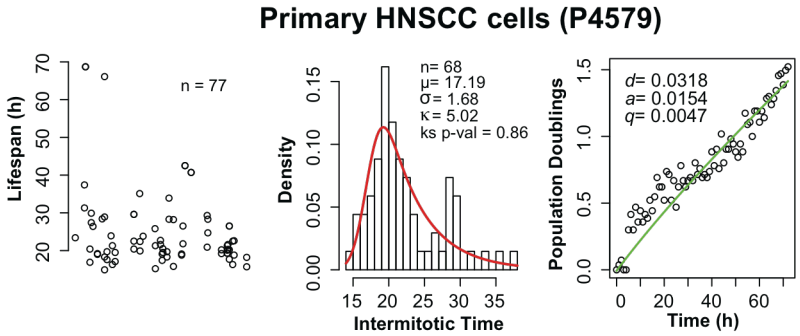

Supplementary Figure 10. **Fractional Proliferation of primary human SCC cells shown in Supplementary Video 3.** Patient-derived tumor cells were isolated from a recurrent squamous cell carcinoma of the tongue. Cells were labeled with recombinant baculoviral particles (CellLight® Nucleus, Invitrogen) at 20 particles per cell, cultured in complete growth medium to obtain exponential growth, and imaged as described for lentiviral-mediated expression. From left to right, the first panel indicates the single cell lifespans, the second is the IMT distribution and the third is the Fractional Proliferation graph. A large number of death events occurred in cells that never divided during the experiment, which was represented by adjusting the death rate. This adjusted death rate together with the division and quiescence rates derived from the data shown in the middle and left panels describes the observed population doublings shown in the right panel.

Supplementary Table 1. **Quiescence-Growth model parameters.**

condition	*d*	*q*	*a*
DMSO	0.0455	0.0050	0.005
1μM	0.0455	0.01550	0.005
4μM	0.0455	0.02063	0.005
16μM	0.0455	0.06217	0.005
16μM*	0.0455	0.04032	0.01295

Supplementary Table 1. **Quiescence-Growth model parameters.** Values shown were fit to the data as described and shown in Supplementary Figure 3. Values for rates of division (*d*), quiescence (*q*) and death (*a*) correspond to the green lines for all conditions (in **Supplementary Fig. 3**), except for 16μM*, which corresponds to the red line.

Supplementary Table 2. **Statistical tests of null hypothesis that the data shown in Supplementary Figure 5 are sampled from the indicated model distribution.**

Model	Test	Statistic	*P*-value
Gaussian	Shapiro-Wilk	W = 0.7511	1.784e-15
log normal	Shapiro-Wilk	W = 0.8915	1.132e-09
inverse normal	Shapiro-Wilk	W = 0.9431	3.318e-06
shifted gamma	ks	D = 0.1644	0.0002532
EMG	ks	D = 0.1012	0.06671

Supplementary Table 2. **Statistical tests of null hypothesis that the data shown in Supplementary Figure 5 are sampled from the indicated model distribution.** An IMT distribution obtained from exponentially proliferating MCF10A cells was fit to the indicated models. All models except the EMG had sufficient evidence to reject them as models describing the distribution (*P*-value less than 0.05). ks, Kolmogorov-Smirnoff test.

Supplementary Table 3. **F-tests of null hypothesis that the EMG model does not provide a better fit than other models.**

Model	MCF10A	AT1	CA1d #1	CA1d #2
Normality	0.0005	0.0001	0.0002	0.0007
Log-Normal	0.0096	0.0015	0.0015	0.0077
Inv-Normal	***0.1167***	0.0027	0.0175	***0.1335***
Gamma	0.0013	0.0000	0.0001	0.0000

Supplementary Table 3. **F-tests of null hypothesis that the EMG model does not provide a better fit than other models.** IMT distributions were obtained from the indicated breast cancer cell lines. Optimal fits of the indicated models to the data were compared to the optimal model fit of an EMG distribution using the F-test; *P*-values are shown. Instances where there is insufficient evidence that the EMG model provides a better fit are indicated in bold. The model of normality (Gaussian) is nested within the EMG model. However, the validity of an F-test comparing the other (non-nested) models is unknown. Inv-Normal, inverse normal distribution.

SUPPLEMENTARY NOTE 1

Mathematical Models

Alternative Quiescence-Growth model containing death rates from both compartments

It is possible that cells die at different rates form each compartment. To accommodate this possibility we have developed an alternative model. Each compartment D and Q are represented by *x* and *y* and have a different death rate (a_d and a_q). This alternative model can be derived as follows:

$$x' = (d - q - a_d)x$$

$$y' = qx - a_q y$$

This is solvable with the following analytical form:

$$x = x_0 e^{(d-q-a_d)t}$$

$$y = \frac{1}{d - q + a_q - a_d} e^{-a_q t}(q\left(x_0\left(e^{(d-q+a_q-a_d)t} - 1\right) - y_0\right) + \left(d + a_q - a_d\right)y_0)$$

If both death rates are equal, the model simplifies to the presented form in the main paper. In our case, the observed death rates were relatively small, and the parameter estimate intervals for each rate overlapped. Therefore, we had insufficient evidence to use the model with different death rates from each compartment and chose, instead, the simpler form described in the main text.

EMG Model of IMT distributions

The non-Gaussian shape of IMT has been reported several decades ago [5], but to our knowledge no standard or customary fit was proposed. To describe the non-Gaussian IMT distributions from single-cell data, we considered several models, including log-normal, inverse-normal and shifted gamma distributions, all of which can fit the consistently observed rightward skew of IMT distributions. Log-normal, inverse-normal (and normal) distribution models routinely failed the Kolmogorov-Smirnoff (ks) one-sided test, with *P* values often less than 10^{-7}, indicating there is sufficient evidence to exclude the model as accurately describing the data. Shifted gamma distributions passed the ks test occasionally, but often failed. The best description of shape for the majority of observed distributions was an Exponentially-Modified Gaussian (EMG) and is described in detail below. An example of testing the various models for fitting the data is shown in Supplementary Figure 6.

The EMG model results from the convolution of a Gaussian (normal) distribution and an exponential distribution. The Gaussian probability density function is described by the following equation with *x* representing the value, and μ the mean and σ the standard deviation.

(eq. 1)

$$g(x;\mu,\sigma) = (2\pi\sigma^2)^{-\frac{1}{2}} e^{-\frac{(x-\mu)^2}{2\sigma^2}}$$

The exponential probability density function is described by the following equation, with *x* representing the value and λ representing the rate.

(eq. 2)

$$h(x;\lambda) = \lambda e^{-\lambda x}, x \geq 0$$

Convolution of these two is simplified to a lower bound of zero due to the boundary condition on the exponential probability density function (and since an intermitotic time must be a positive value).

(eq. 3)

$$f(x;\mu,\sigma,\lambda) = (g * h)(x) = \int_0^\infty g(x-y)h(y)dy$$

This results in the following analytic form of the EMG probability density function.

(eq. 4)

$$f(x;\mu,\sigma,\lambda) = \frac{\lambda}{2} e^{\frac{\lambda}{2}(-2x+2\mu+\lambda\sigma^2)} erfc\left(\frac{-x+\mu+\lambda\sigma^2}{\sigma\sqrt{2}}\right)$$

Note that the meaning of the parameters of the EMG distribution has changed from that of its parts, *e.g.* μ no longer represents the mean of the distribution. A functional application of this work has been published in the R code repository (http://r-project.org) and can be viewed and used by calling the 'emg' package (http://cran.r-project.org/web/packages/emg/emg.pdf).

Calculation of division rate from EMG

The division rate for cells undergoing exponential growth is usually approximated by the natural logarithm of 2 divided by the mean division time. As shown above, however, IMT distributions are non-Gaussian and the mean cannot accurately represent the population when the distribution deviates substantially from normality. A probability method that accounts for the effects of heterogeneity in estimating division rate (*d*) of dividing bacteria has been described. [3] We substituted the EMG distribution in place of the Pearson Type III distribution used in the original formulation (equation 10 in reference [3]), which results in the following formula to be solved for the division rate (*d*):

(eq. 5)

$$2\int_0^\infty e^{-dt} EMG(\tau|\mu,\sigma,\lambda)d\tau = 1$$

EMG is a statistical model with three forms: probability density, cumulative and survival. Each one of these functions considers all EMG parameters. Using estimates for μ, σ, and λ obtained from EMG model fits to IMT distributions, the division rate, *p*, is obtained by solving for the root. This calculation is performed by the function `generation.rate` in the R code shown below. Moreover, the estimation of quiescence requires the survival function of the EMG and relies on all parameters.

Likelihood of Quiescence model

Estimation of the number of cells that reach the end of an experiment (EoE) that are quiescent was determined using a likelihood model and survival analysis. The survival function describes the probability that a cell reaching the EoE would have divided if more time were observed. The likelihood formula uses both the complete lifespans obtained from divided cells (*i*) and the censored lifespan information from cells reaching the EoE (*j*). By definition, the likelihood function is the conditional probability of the data given the parameters of the model. The likelihood function is defined as the product of the likelihood of each datum The dividing cell population is represented by an EMG model (*f* for probability density and *F* for cumulative distribution), the fixed percentage of quiescent cells is represented by *q*, the information of observed divisions is represented by *i* and lifespans without observed division represented by *j*.

(eq. 6)

$$\prod\prod f(x_i, y_i|\mu,\sigma,\lambda) = \prod_i (1-q) f(x_i|\mu,\sigma,\lambda) \prod_j q + (1-q)(1-F(y_j|\mu,\sigma,\lambda))$$

The first product is the standard likelihood estimate, modified by the fraction of dividing cells (1-*q*). The second product is the likelihood that a cell is quiescent (*q*) multiplied by the chance that it was going to divide later (1-*F*). The model output is the fraction of quiescent cells present in the observed single-cell lifespan data and can be fit by maximizing the negative log likelihood using the `emg3.mle` function in the `fracprolif` R package. The data are passed to this function as a list of observed `Lifespans` (in hours) and whether the observation persisted to the EoE (`TRUE` for cells that reach the EoE). See Computational tools below for further details.

Calculating the rate of entry into quiescence

Once the division rate and the fraction of quiescent cells are calculated, it is possible to derive a rate of entry into quiescence. Each rate represents the number of expected events (divisions or transitions into quiescence) divided by the total observation time.

$$d = \frac{\text{divisions}}{\text{observation time in D}} \qquad q = \frac{\text{transitions into quiescence}}{\text{observation time in P}}$$

Total observation time in this example extends to a continuous model.

The conceptual diagram of the two compartments of a cell population, dividing (D) and non-dividing (Q), is shown with the rates of transition between them in Figure 2 of the main text, and Figure 3 illustrates the data used in likelihood estimation, including the observed lifespan of the cells and the parameters of the EMG model fit to the IMT distribution. The total cell observation time (the sum of lifespans of all cell observed) of the D compartment in the experiment is not explicit, as it includes all the observations of cells that divided and some fraction of the observations at the end of experiment. However, the actual observation time of cells in the D compartment is not required, as it will cancel out. Both rates are defined relative to the D compartment, *i.e.* both arrows in Fig. 3 relate to exit from the D compartment and, thus, the relevant cell observation times for both rates are the same. It follows that the count of events (c) in each compartment at the end of an experiment with observation time (o_t) is:

$$c_d = do_t \qquad c_q = qo_t$$

The fraction of quiescence events (f_Q) observed at end of experiment is defined as:

$$f_Q = \frac{c_q}{c_d + c_q}$$

The observation time cancels, and the following equation results:

$$f_Q = \frac{q}{d + q}$$

Solving for the unknown rate of quiescence results in the following transform:

$$q = \frac{f_Q}{1 - f_Q} d$$

As shown, the rate of quiescence is calculated based on the fraction of quiescent cells and the rate of division.

SUPPLEMENTARY NOTE 2

Computational tools

Mathematica[11] was used for generating the interactive Mathematica CDF Player file (**Supplementary Software 1**) and the surface plots in **Supplementary Figure 1**.

The freely available ImageJ[12,13] software (http://rsb.info.nih.gov/ij/) was used for image analysis (manual single-cell tracking and automated cell counting by enumeration of nuclei).

The freely available statistical software package R[14] (http://www.R-project.org) was used for statistical tests and data analyses and to develop the `fracprolif` package (R extension).

Basic description of the `fracprolif` package

We have developed an extension of R that incorporates all of the code used to analyze single-cell and population-level proliferation data and generate Fractional Proliferation Graphs. The package is called `fracprolif` and must be installed into the R framework in order to use it. The `fracprolif` package contains two sample data files, all of the functions for performing the analyses, and manual pages (description files) for the entire package. For those familiar with R, detailed information is provided within the package itself by typing the following into the R console:

```
?fracprolif
```

A step-by-step guide to generating data appropriately structured for analysis by `fracprolif`

Single-cell data

Single-cell data are obtained by manually tracking individual cells from an image stack (here we use H2BmRFP-expressing cells; cell culture and imaging techniques are described in Methods). ImageJ, or any software capable of opening the entire image series as a stack and advancing frame by frame, is used for the manual tracking. Individual cells are followed across frames and observed cell lifespans are recorded. Each cell lifespan is defined by a start event (mitosis) and an end event (mitosis, death or end of experiment). Start events are shared among siblings (sister cells) and assigned an identifier comprised of the frame number and a letter. End events are assigned an identifier of frame number and a letter if mitotic. In some cases a mitotic end event identifier corresponds to another start event identifier (indicative of cell progeny). Events are converted to time units based on the frame acquisition rate (sampling interval), and cell birth time and lifespan are expressed in hours. The steps performed to record the single cell data are as follows:

1. When a mitotic event occurs, the daughter cells are each assigned the next rows available in the data file
2. The frame number of the event is recorded in the `Birth.frame` column of the rows assigned in (1).
3. The event from (1) is given an alphabetic identifier not previously used within the same `Birth.frame`.
4. The last frame a cell is observed in is recorded in the `End.frame`.
5. If the last frame is a mitotic event, assign letter as (3) in `End.ID`.
6. If the cell is present in the last frame of the image stack, the column `End.of.Expt` is marked `TRUE`, otherwise it is marked `FALSE`.
7. If a cell is observed to die, this is recorded in the column `Death` as `TRUE`, otherwise as `FALSE`.
8. Create `Birthtime` column in hours by dividing `Birth.frame` by the sampling rate (e.g. 5 images per hour).
9. Create `Lifespan` column in hours by dividing (`End.frame` - `Birth.frame`) by the sampling rate.

A movie demonstrating the manual labeling is provided as Supplementary Movie 2 and an example data set is provided within the `fracprolif` package.

To load the data set, type the following command in the R console: `data(ca1d.erlotinib)`

To view the column names and the first few rows of data, type: `head(ca1d.erlotinib)`

The complete raw data can be viewed by typing: `ca1d.erlotinib`

Population-level data

Cell counts are obtained from the same image stack as for single-cell tracking except that the sampling rate is once per hour. The image stack is opened in ImageJ and automatically processed using the following steps: 1) threshold the images and convert them to binary, 2) reduce undersegmentation by performing a watershed algorithm, and 3) identify the objects (nuclei) within each image. The ImageJ macro used to perform these steps is shown here:

```
// ImageJ macro for nuclei enumeration
// Written by Darren R. Tyson, 2009

run("Subtract Background...", "rolling=50 stack");
setThreshold(14, 4000);
run("Convert to Mask", " ");
run("Watershed", "stack");
run("Analyze Particles...", "size=150-4000 circularity=0.20-1.00 show=Outlines clear exclude
   include summarize stack");
```

The object counts obtained from the ImageJ macro are stored in a column for each image stack and counts from replicate conditions (within a single experiment) are summed and converted to log2 scale for each unit of time (in this case every hour). An example data set of total cell counts was generated from the same experiment in which the single-cell data described above was obtained and is provided with the `fracprolif` package in R. The data can be loaded by typing the following command in the R console:

```
data(ca1d.erlotinib.totals)
```

Time (in hours) is provided in the first column and cell counts obtained in the presence of various concentrations of erlotinib (indicated by the column name, e.g. `e_16000` for 16 μM erlotinib) are provided in the remaining columns.

Cut-and-paste code to produce the Fractional Proliferation Graphs shown in Figure 3*f*.

Using the two data sets described above, the graphs shown in Figure 3*f* can be generated by copying and pasting all of the code below into the R console. (Note that the code can be copied and pasted piecewise, if necessary, and is also available in a separate file, **Supplementary Software 2**.)

```
#          Load the data
###################################
data(ca1d.erlotinib)
data(ca1d.erlotinib.totals)

#        Process the data
###################################
mitotic.lifespans <- subset(ca1d.erlotinib,  !End.of.Expt  &
                                             !Death        &
                                             !is.na(Lifespan))$Lifespan

censored.lifespans <- subset(ca1d.erlotinib, End.of.Expt   &
                                             !Death        &
                                             !is.na(Lifespan))$Lifespan
est <- q.mle.emg.estimate(mitotic.lifespans, censored.lifespans)
r <- q.rates("emg", est)
m <- lm(DMSO ~ Time_h, ca1d.erlotinib.totals)
untreated.division.rate <- coef(m)['Time_h']*log(2)
half.imt <- log(2)/untreated.division.rate/2
y <- ca1d.erlotinib.totals$e_16000 - ca1d.erlotinib.totals$e_16000[1]
t <- ca1d.erlotinib.totals$Time_h
fit <- nls(y ~ log(split_tot(t, 1, 0,
                             untreated.division.rate, r['d'],
                             0.0, r['q'],
                             0.0, 0.0, a, a,
                             half.imt), 2),
           start=list(a=0.003),
           lower=list(a=0),
           algorithm="port")
a <- coef(fit)
```

```
#      Plot the data
############################
dev.new(width=7, height=3)
par(mfrow=c(1,3))
d <- subset(ca1d.erlotinib, !Death & !is.na(Lifespan))

#    Birthtime vs Lifespan plot
###################################
plot(d$Birthtime,
     d$Lifespan,
     main="CA1d 16μM erlotinib",
     xlab="Birth time (h)",
     ylab="Lifespan (h)",
     ylim=c(5,90), xlim=c(0,25))
n <- length(d$Lifespan)
text(20,80,substitute("n" == n,list(n=n)))
p <- 100*length(subset(d, End.of.Expt)$Lifespan) / n
text(15,85,substitute(p * "% EoE", list(p=round(p))))

#   Intermitotic Time Histogram
###################################
hist(mitotic.lifespans,
     main='CA1d 16μM erlotinib',
     xlab="Observed Intermitotic Times (h)",
     breaks=20,
     freq=FALSE)
curve(demg(x, coef(est)['mu'],
           coef(est)['sigma'],
           coef(est)['lambda']),
           add=TRUE, col='red', lwd=2)
text(35, 0.07,  pos=4, labels=substitute("n"==n, list(n=length(mitotic.lifespans))))
text(35, 0.065, pos=4, labels=substitute(mu==m, list(m=round(coef(est)['mu'],2))))
text(35, 0.06,  pos=4, labels=substitute(sigma==s, list(s=round(coef(est)['sigma'],2))))
text(35, 0.055, pos=4, labels=substitute(kappa==l, list(l=round(1/coef(est)['lambda'],2))))
ks <- ks.test(mitotic.lifespans, "pemg",
              mu=coef(est)['mu'],
              sigma=coef(est)['sigma'],
              lambda=coef(est)['lambda'])
text(35, 0.05, pos=4, labels=substitute("ks p-val"==p, list(p=round(ks$p.value,2))))

#  Fractional Proliferation Graph
###################################
plot (t, y,
      main="CA1d 16μM erlotinib",
      xlab="Time (h)",
      ylab="Population Doublings",
      ylim=c(0,1.5))

model.total <- log(split_tot(t, 1, 0, untreated.division.rate,
                             r['d'], 0.0, r['q'], 0, 0,
                             a['a'], a['a'], half.imt), 2)
lines(t,model.total,col="green")
lines(t,model.total*split_fq(t, 1, 0, untreated.division.rate,
                             r['d'], 0.0, r['q'], 0, 0,
                             a['a'], a['a'], half.imt), col="red")
lines(t,model.total*split_fd(t, 1, 0, untreated.division.rate,
                             r['d'], 0.0, r['q'], 0, 0,
                             a['a'], a['a'], half.imt), col="blue")
text(2, 1.4, pos=4, substitute("d" == d, list(d=round(r['d'], 4))))
text(2, 1.3, pos=4, substitute("q" == q, list(q=round(r['q'], 4))))
text(2, 1.2, pos=4, substitute("a" == a, list(a=round(a['a'], 4))))
```

SUPPLEMENTARY NOTE 3

Orthogonal assays of erlotinib-induced PC9 cell quiescence

To our knowledge, there is no known positive marker of quiescent cells, but low Ki-67 expression is a *de facto* surrogate [4]. By flow cytometry the fraction of Ki-67^{low} PC9 cells increased over time in response to erlotinib in a similar fashion to the increase in the quiescent cell fraction predicted from the integrated model (**Supplementary Fig. 7a**). In additional independent assays, cells were fixed after various times of treatment with erlotinib and stained by indirect immunofluorescence for Ki-67 (**Supplementary Fig. 7b**,**c**) or p27^{Kip1}, a known inhibitor of cell cycle progression [15]. The fractions of Ki-67^{low} cells were similar to the quiescent fraction determined using the integrated model. Conversely, the levels of p27 increased in response to erlotinib treatment (reference [16] and not shown). Thus, these separate assays all indicate that PC9 cells enter quiescence in response to erlotinib. In addition, A375 cells (an oncogene-addicted melanoma cell line expressing V600E B-Raf [10]) treated with the Raf inhibitor PLX-4720 (**Supplementary Fig. 1d**) increase their expression and nuclear localization of p27Kip1 (**Supplementary Fig. 8**), further supporting the relationship between G1 arrest and nonlinear proliferation rates.

LITERATURE CITED IN SUPPLEMENTARY INFORMATION

1. Gong, Y.*, et al.* Induction of BIM is essential for apoptosis triggered by EGFR kinase inhibitors in mutant EGFR-dependent lung adenocarcinomas. *PLoS Med.* **4**, e294 (2007).
2. Sharma, S.V.*, et al.* A chromatin-mediated reversible drug-tolerant state in cancer cell subpopulations. *Cell* **141**, 69-80 (2010).
3. Powell, E.O. Growth rate and generation time of bacteria, with special reference to continuous culture. *J. Gen. Microbiol.* **15**, 492-511 (1956).
4. Scholzen, T. & Gerdes, J. The Ki-67 protein: from the known and the unknown. *Journal of Cellular Physiology* **182**, 311-322 (2000).
5. Kubitschek, H.E. The distribution of cell generation times. *Cell Tissue Kinet* **4**, 113-122 (1971).
6. Soule, H.D.*, et al.* Isolation and characterization of a spontaneously immortalized human breast epithelial cell line, MCF-10. *Cancer Res.* **50**, 6075-6086 (1990).
7. Dawson, P.J., Wolman, S.R., Tait, L., Heppner, G.H. & Miller, F.R. MCF10AT: a model for the evolution of cancer from proliferative breast disease. *Am J Pathol* **148**, 313-319 (1996).
8. Santner, S.J.*, et al.* Malignant MCF10CA1 cell lines derived from premalignant human breast epithelial MCF10AT cells. *Breast cancer research and treatment* **65**, 101-110 (2001).
9. Kasid, U., Pfeifer, A., Weichselbaum, R.R., Dritschilo, A. & Mark, G.E. The raf oncogene is associated with a radiation-resistant human laryngeal cancer. *Science* **237**, 1039-1041 (1987).
10. Tsai, J.*, et al.* Discovery of a selective inhibitor of oncogenic B-Raf kinase with potent antimelanoma activity. *Proc. Natl. Acad. Sci. U. S. A.* **105**, 3041-3046 (2008).
11. Wolfram Research Inc. Mathematica. (Champaign, IL, 2010).
12. Abramoff, M.D., Magalhaes, P.J. & Ram, S.J. Image Processing with ImageJ. *Biophotonics International* **11**, 36–42 (2004).
13. Rasband, W.S. ImageJ. (U. S. National Institutes of Health, Bethesda, Maryland, 1997–2012).
14. R Development Core Team. R: A language and environment for statistical computing. R Foundation for Statistical Computing. (Vienna, Austria, 2010).
15. Chu, I.M., Hengst, L. & Slingerland, J.M. The Cdk inhibitor p27 in human cancer: prognostic potential and relevance to anticancer therapy. *Nat. Rev. Cancer* **8**, 253-267 (2008).
16. Ling, Y.H.*, et al.* Erlotinib, an effective epidermal growth factor receptor tyrosine kinase inhibitor, induces p27KIP1 up-regulation and nuclear translocation in association with cell growth inhibition and G1/S phase arrest in human non-small-cell lung cancer cell lines. *Mol. Pharmacol.* **72**, 248-258 (2007).